DOCK5 functions as a key signaling adaptor that links FcεRI signals to microtubule dynamics during mast cell degranulation

Kana Ogawa,[1,3] Yoshihiko Tanaka,[1,2,3] Takehito Uruno,[1,3] Xuefeng Duan,[2,3] Yosuke Harada,[1,3] Fumiyuki Sanematsu,[1,2,3] Kazuhiko Yamamura,[1,3] Masao Terasawa,[1,3] Akihiko Nishikimi,[1,2,3] Jean-François Côté,[4] and Yoshinori Fukui[1,2,3]

[1]Division of Immunogenetics, Department of Immunobiology and Neuroscience and [2]Research Center for Advanced Immunology, Medical Institute of Bioregulation, Kyushu University, Fukuoka 812-8582, Japan
[3]Core Research for Evolutional Science and Technology (CREST), Japan Science and Technology Agency, Tokyo 102-0076, Japan
[4]Institut de Recherches Cliniques de Montréal, Université de Montréal, Montréal, Quebec H2W 1R7, Canada

Mast cells play a key role in the induction of anaphylaxis, a life-threatening IgE-dependent allergic reaction, by secreting chemical mediators that are stored in secretory granules. Degranulation of mast cells is triggered by aggregation of the high-affinity IgE receptor, FcεRI, and involves dynamic rearrangement of microtubules. Although much is known about proximal signals downstream of FcεRI, the distal signaling events controlling microtubule dynamics remain elusive. Here we report that DOCK5, an atypical guanine nucleotide exchange factor (GEF) for Rac, is essential for mast cell degranulation. As such, we found that DOCK5-deficient mice exhibit resistance to systemic and cutaneous anaphylaxis. The Rac GEF activity of DOCK5 is surprisingly not required for mast cell degranulation. Instead, DOCK5 associated with Nck2 and Akt to regulate microtubule dynamics through phosphorylation and inactivation of GSK3β. When DOCK5–Nck2–Akt interactions were disrupted, microtubule formation and degranulation response were severely impaired. Our results thus identify DOCK5 as a key signaling adaptor that orchestrates remodeling of the microtubule network essential for mast cell degranulation.

CORRESPONDENCE
Yoshinori Fukui:
fukui@bioreg.kyushu-u.ac.jp

Abbreviations used: BMMC, BM-derived mast cell; c-APC, C-terminal fragment of adenomatous polyposis coli; CBB, Coomassie brilliant blue; DNFB, dinitrofluorobenzene; GEF, guanine nucleotide exchange factor; GST, glutathione *S*-transferase; HSA, human serum albumin; PI3K, phosphatidylinositol 3-kinase; PIP_3, phosphatidylinositol 3,4,5-triphosphate; RSK, ribosomal S6 kinase; S6K, p70 S6 kinase; WASP, Wiskott-Aldrich syndrome protein; WIP, WASP-interacting protein.

Mast cells play a key role in induction of anaphylaxis, a life-threatening allergic reaction which occurs rapidly after exposure of certain antigens, such as foods, drugs, and insect venoms (Sampson et al., 2005). Mast cells express the high-affinity receptor for IgE, FcεRI, on their surface, and binding of multivalent antigens to FcεRI-bound IgE induces receptor aggregation and triggers mast cell activation (Kawakami and Galli, 2002; Kraft and Kinet, 2007). Activated mast cells secrete preformed chemical mediators, including proteases and vasoactive amines such as histamine, which are stored in cytoplasmic secretory granules (Kawakami and Galli, 2002; Lundequist and Pejler, 2011). This process involves the movement of secretory granules and their fusion with the plasma membrane followed by exocytosis to release the chemical mediators (Blott and Griffiths, 2002; Lundequist and Pejler, 2011). Degranulation of mast cells is therefore a complex and multistep process that is tightly regulated by FcεRI-mediated signals.

Upon aggregation of FcεRI with IgE and antigens, two parallel signaling cascades operate. One cascade is initiated by activation of the Src family protein tyrosine kinase Lyn, which is bound to the FcεRI β subunit, and involves subsequent activation of the nonreceptor protein tyrosine kinase Syk (Kawakami and Galli, 2002; Kraft and Kinet, 2007; Alvarez-Errico et al., 2009; Gilfillan and Rivera, 2009; Kambayashi et al., 2009). The activated Syk then phosphorylates multiple substrates, including PLC-γ (Kawakami and Galli, 2002; Kraft and Kinet,

The Rockefeller University Press $30.00
J. Exp. Med. 2014 Vol. 211 No. 7 1407-1419
www.jem.org/cgi/doi/10.1084/jem.20131926

The Journal of Experimental Medicine

2007; Alvarez-Errico et al., 2009; Gilfillan and Rivera, 2009; Kambayashi et al., 2009). The other cascade uses Fyn, another FcεRI-associated Src family protein tyrosine kinase (Kraft and Kinet, 2007; Alvarez-Errico et al., 2009; Gilfillan and Rivera, 2009; Kambayashi et al., 2009). Fyn phosphorylates the adaptor protein Gab2, which leads to activation of phosphatidylinositol 3-kinase (PI3K) through association with the p85α regulatory subunit (Gu et al., 2001; Parravicini et al., 2002; Nishida et al., 2005, 2011). Several lines of evidence indicate that although the Lyn–Syk–PLC-γ axis regulates granule-plasma membrane fusion and exocytosis by controlling calcium response (Nishida et al., 2005; Alvarez-Errico et al., 2009; Gilfillan and Rivera, 2009; Kambayashi et al., 2009), the Fyn–Gab2 pathway plays a key role in translocation of secretory granules to the plasma membrane (Parravicini et al., 2002; Nishida et al., 2005, 2011). However, little is known about the distal events controlling mast cell degranulation. In particular, movement of secretory granules requires dynamic rearrangement of microtubules (Martin-Verdeaux et al., 2003; Smith et al., 2003; Nishida et al., 2005; Dráber et al., 2012), yet the signaling events regulating this step of mast cell activation are poorly understood.

GSK3β is a serine/threonine kinase that negatively regulates microtubule dynamics (Cohen and Frame, 2001; Zhou and Snider, 2005). In resting cells, GSK3β phosphorylates many microtubule-binding proteins and inhibits their ability to interact with microtubules and to promote microtubule assembly (Zhou et al., 2004; Yoshimura et al., 2005; Kim et al., 2011). This inhibitory effect is relieved when GSK3β is phosphorylated at serine residue of position 9 (Ser9; Cohen and Frame, 2001). Although knockdown experiments revealed a role for GSK3β in cytokine production, chemotaxis, and survival of human mast cells (Rådinger et al., 2010; Rådinger et al., 2011), aggregation of FcεRI also induces GSK3β phosphorylation at Ser9 (Rådinger et al., 2010). Therefore, phosphorylation-dependent inactivation of GSK3β may be involved in FcεRI-mediated regulation of microtubule dynamics in mast cells.

DOCK5 is a member of the atypical guanine nucleotide exchange factors (GEFs) for the Rho family of GTPases (Côté and Vuori, 2002). Although DOCK5 does not contain the Dbl homology domain typically found in GEFs (Schmidt and Hall, 2002), DOCK5 mediates the GTP–GDP exchange reaction for Rac through DOCK homology region 2 (DHR-2; also known as CZH2 or Docker) domain (Brugnera et al., 2002; Côté and Vuori, 2002; Meller et al., 2002). DOCK5 is widely expressed in various tissues and regulates multiple cellular functions, including myoblast fusion and bone resorption (Laurin et al., 2008; Vives et al., 2011), yet its roles in the immune system and immune responses remain unexplored. In this study, we demonstrate that DOCK5 regulates FcεRI-mediated anaphylactic responses in vivo and mast cell degranulation in vitro. Unexpectedly, this regulation by DOCK5 does not require its Rac GEF activity, but instead involves association with Nck2 and Akt. When this interaction was blocked in mast cells, FcεRI-mediated phosphorylation and inactivation of GSK3β were impaired, resulting in a marked reduction in microtubule dynamics and a severe defect in degranulation. Our results thus define a novel regulatory mechanism controlling degranulation response in mast cells.

RESULTS

DOCK5, but not DOCK2, is required for induction of anaphylactic responses in vivo

DOCK proteins constitute a family of evolutionarily conserved GEFs for the Rho family of GTPases. This family consists of 11 members and is further classified into four subfamilies (DOCK-A, -B, -C, and -D) based on their sequence homology and substrate specificity (Côté and Vuori, 2002). DOCK-A subfamily proteins, including DOCK1 (also known as DOCK180), DOCK2, and DOCK5, act as Rac-specific GEFs in varied biological settings (Kiyokawa et al., 1998; Fukui et al., 2001; Côté and Vuori, 2002, 2006; Sanui et al., 2003; Kunisaki et al., 2006; Gotoh et al., 2010; Sanematsu et al., 2013). To investigate whether DOCK-A GEFs are involved in regulation of mast cell functions, we analyzed their expressions in mast cells. Western blot analysis revealed that mast cells express DOCK2 and DOCK5, but not DOCK1 (not depicted). As mast cells are important for induction of IgE-mediated allergic responses, we first examined the potential function of these Rac GEFs in systemic anaphylaxis by using the knockout mice that had been backcrossed onto a C57BL/6 background for more than eight generations. For this purpose, we passively sensitized mice with anti-DNP IgE antibody 24 h before intravenous administration of DNP–human serum albumin (HSA). When sensitized WT C57BL/6 mice were challenged with DNP-HSA, they exhibited a progressive decrease in rectal temperature to 3.2°C below the basal level by 15 min (Fig. 1 A). Similar results were obtained when DOCK2-deficient (*Dock2*$^{-/-}$) mice were similarly treated with DNP-HSA (Fig. 1 A). Surprisingly, however, rectal temperature was only modestly affected in DOCK5-deficient (*Dock5*$^{-/-}$) mice (Fig. 1 A). Consistent with this finding, *Dock5*$^{-/-}$ mice, compared with WT and *Dock2*$^{-/-}$ mice, exhibited a marked reduction in serum concentration of histamine (Fig. 1 B).

To further investigate the role of DOCK5 in allergic responses in vivo, we next examined cutaneous anaphylaxis in mice sensitized with anti-DNP IgE antibody. When WT and *Dock2*$^{-/-}$ mice were challenged by epicutaneous application of dinitrofluorobenzene (DNFB) in acetone and olive oil in the left ear, the thickness of the left ear markedly increased by 6.5 h, as compared with that of the right ear treated with vehicle alone (Fig. 1 C). However, the ear swelling in response to DNFB stimulation was reduced macroscopically and histologically in *Dock5*$^{-/-}$ mice (Fig. 1, C and D). Toluidine blue staining and flow cytometric analysis revealed that normal numbers of mast cells exist in the ear, stomach, and peritoneal cavity of *Dock5*$^{-/-}$ mice (Fig. 1, E and F). Collectively, these results indicate that DOCK5 deficiency renders mice resistant to systemic and cutaneous anaphylaxis without affecting mast cell development.

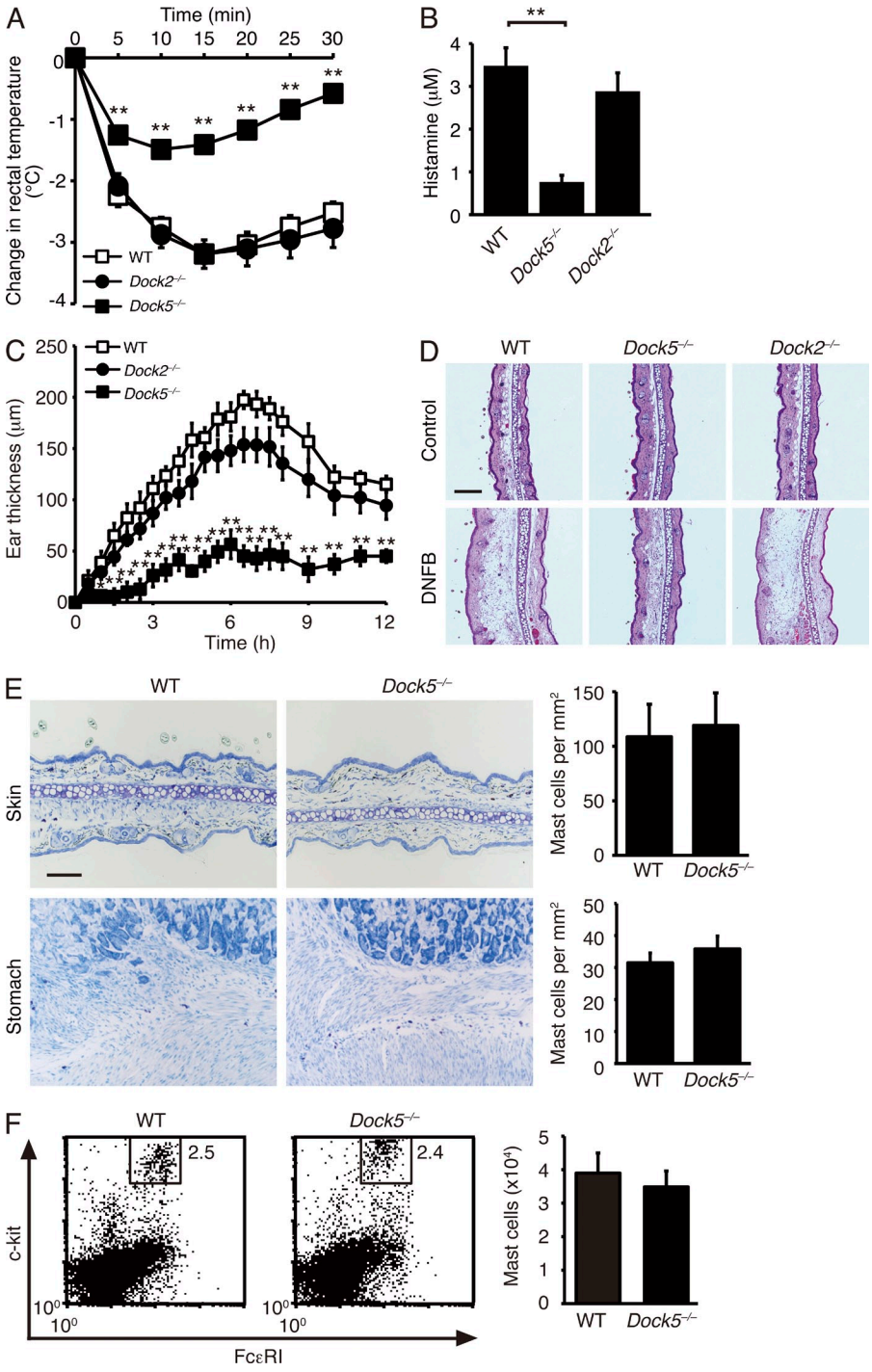

Figure 1. DOCK5, but not DOCK2, is required for induction of systemic and cutaneous anaphylaxis. (A) The change of rectal temperature in WT ($n = 17$), *Dock2*$^{-/-}$ ($n = 12$), and *Dock5*$^{-/-}$ ($n = 18$) mice sensitized with anti-DNP IgE antibody and then challenged 24 h later with DNP-HSA. (B) Serum concentrations of histamine in WT ($n = 4$), *Dock2*$^{-/-}$ ($n = 6$), and *Dock5*$^{-/-}$ ($n = 6$) mice treated as in A. (C) Ear swelling of WT ($n = 9$), *Dock2*$^{-/-}$ ($n = 9$), and *Dock5*$^{-/-}$ ($n = 9$) mice sensitized with anti-DNP IgE antibody and then challenged 24 h later by epicutaneous application of DNFB in acetone and olive oil (left ear) or vehicle alone (right ear). Ear swelling was calculated as the difference between the thickness of the left and right ear. (A–C) Data were collected from seven (A), six (B), or three (C) separate experiments and are indicated as mean ± SEM; *, $P < 0.05$; **, $P < 0.01$. (D) Histological sections of the right ears (control) and left ears (DNFB) stained with hematoxylin and eosin. Representative data of nine mice per group are shown. (E) Toluidine blue staining of the ear skin and stomach from WT and *Dock5*$^{-/-}$ mice. For each tissue, the number of mast cells per square millimeter is compared between WT and *Dock5*$^{-/-}$ mice (mean ± SD; $n = 3$). Bars: (D) 200 μm; (E) 100 μm. (F) Flow cytometric analysis for peritoneal mast cells from WT and *Dock5*$^{-/-}$ mice. The numeral in the square indicates the percentage of mast cells for total peritoneal exudate cells. The number of peritoneal mast cells is compared between WT and *Dock5*$^{-/-}$ mice (mean ± SD; $n = 3$). (E and F) Data are representative of two independent experiments.

DOCK5 acts in mast cells and regulates anaphylactic responses in vivo

Mast cells can be differentiated from BM cells in vitro by treatment with IL-3. When the expression levels of mast cell developmental markers c-kit and FcεRI were compared, no significant difference was found between WT and *Dock5*$^{-/-}$ BM-derived mast cells (BMMCs; Fig. 2 A). Similarly, mast cell–specific proteases such as mMCP5, mMCP6, and MC-CPA were normally expressed in *Dock5*$^{-/-}$ BMMCs (Fig. 2 B; Morii et al., 1997). In addition, we found that DOCK5 deficiency does not affect survival of mast cells in vitro (not depicted). To confirm whether DOCK5 plays a specific role in mast cells during anaphylactic responses, we injected WT and *Dock5*$^{-/-}$ BMMCs intravenously into *Kit*$^{W\text{-}sh/W\text{-}sh}$ C57BL/6 mice, which are devoid of mast cells in multiple anatomical sites at 10 wk old (Grimbaldeston et al., 2005; Wolters et al., 2005). 11 wk after intravenous injection, comparable numbers of WT and *Dock5*$^{-/-}$ BMMCs were

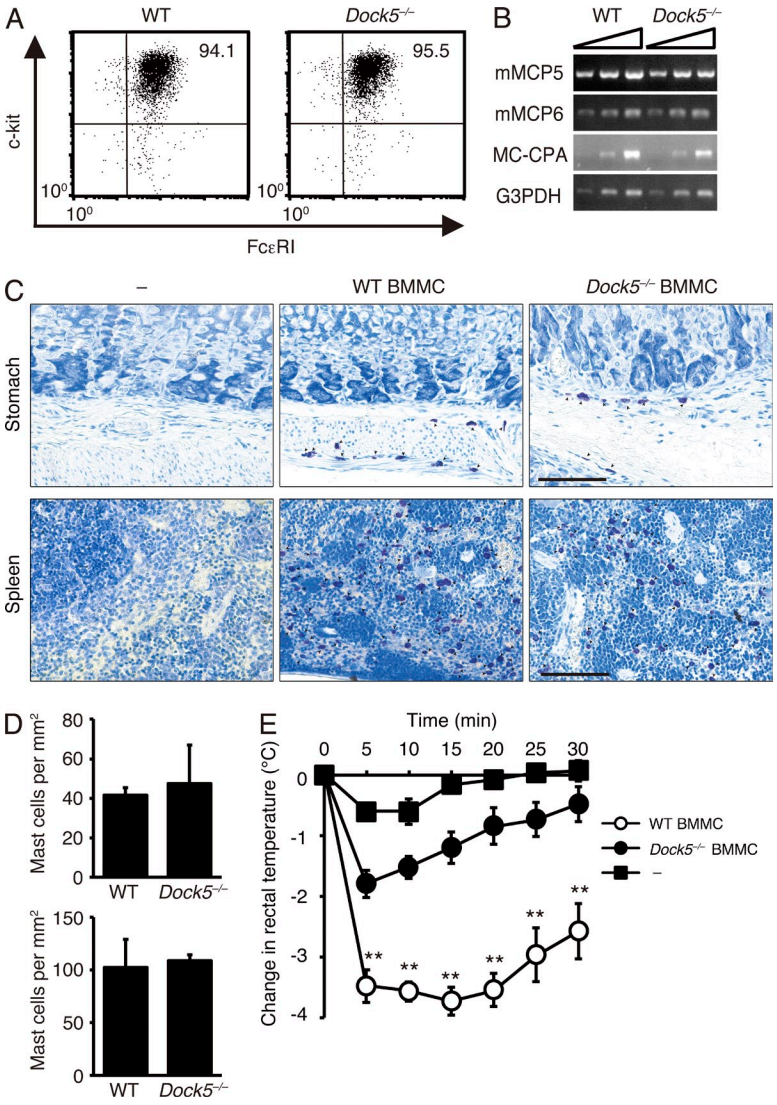

Figure 2. DOCK5 acts in mast cells and regulates anaphylactic responses in vivo. (A) Cell surface expression of c-kit and FcεRI on WT and *Dock5*$^{-/-}$ BMMCs was measured by flow cytometry. Data are representative of 10 independent experiments. (B) mRNA expression of mast cell–specific proteases in WT and *Dock5*$^{-/-}$ BMMCs was determined by RT-PCR. Data are representative of two independent experiments. (C) Toluidine blue staining of the stomach and spleen from the *Kit*$^{W\text{-}sh/W\text{-}sh}$ C57BL/6 mice reconstituted with WT and *Dock5*$^{-/-}$ BMMCs. The arrowheads indicate mast cells. Data are representative of four mice per group collected from two independent experiments. The data on nontreated *Kit*$^{W\text{-}sh/W\text{-}sh}$ mice are shown as controls (–). Bar, 100 µm. (D) Comparison of the number of mast cells in the stomach (top) and spleen (bottom) from the *Kit*$^{W\text{-}sh/W\text{-}sh}$ C57BL/6 mice reconstituted with WT and *Dock5*$^{-/-}$ BMMCs (n = 4 mice per group) was made from histological analysis as in C. Data were collected from two separate experiments and are indicated as mean ± SD. (E) The change of rectal temperature in *Kit*$^{W\text{-}sh/W\text{-}sh}$ C57BL/6 mice receiving WT (n = 6) or *Dock5*$^{-/-}$ (n = 7) BMMCs. Nontreated *Kit*$^{W\text{-}sh/W\text{-}sh}$ mice (n = 3) were also analyzed as controls (–). Mice were sensitized with anti-DNP IgE antibody and then challenged 24 h later with DNP-HSA. Data were collected from three separate experiments and are indicated as mean ± SEM; **, $P < 0.01$.

found in the stomach and spleen, indicating that DOCK5 deficiency does not affect engraftment of transferred mast cells (Fig. 2, C and D). However, although *Kit*$^{W\text{-}sh/W\text{-}sh}$ mice receiving WT BMMCs exhibited a marked decrease in rectal temperature upon stimulation (Fig. 2 E), administration of *Dock5*$^{-/-}$ BMMCs failed to effectively induce systemic anaphylaxis in *Kit*$^{W\text{-}sh/W\text{-}sh}$ mice (Fig. 2 E). These results indicate that DOCK5 acts in mast cells and regulates systemic anaphylaxis in vivo.

DOCK5 regulates mast cell degranulation by controlling microtubule dynamics

To determine the precise role of DOCK5 in mast cells, we sensitized WT and *Dock5*$^{-/-}$ BMMCs with anti-DNP IgE antibody in vitro and then stimulated them with varying doses of DNP-HSA. Upon stimulation, WT BMMCs released considerable amounts of β-hexosaminidase, a protein stored in secretory granules (Fig. 3 A). However, FcεRI-mediated β-hexosaminidase release was severely impaired in *Dock5*$^{-/-}$ BMMCs (Fig. 3 A), in spite of the fact that the total amount of β-hexosaminidase was comparable between WT and *Dock5*$^{-/-}$ BMMCs (see Materials and methods). Similar results were obtained when histamine release was analyzed (Fig. 3 B). In contrast, DOCK5 deficiency did not affect FcεRI-mediated production of IL-6 and IL-13 by BMMCs (Fig. 3, C and D). In addition, the release of lipid mediators such as prostaglandin D_2 and leukotriene C_4 were unchanged between WT and *Dock5*$^{-/-}$ BMMCs (Fig. 3, E and F). These results indicate that DOCK5 selectively regulates degranulation response during FcεRI-mediated mast cell activation.

The secretory granules of mast cells possess several proteins present almost exclusively in lysosomes in nonhematopoietic cells, and for this reason, these organelles have been referred to as secretory lysosomes (Blott and Griffiths, 2002). We examined intracellular trafficking of secretory granules by visualizing them with LysoTracker. Before stimulation with DNP-HSA, LysoTracker-positive secretory granules were found in cytoplasm in both WT and *Dock5*$^{-/-}$ BMMCs

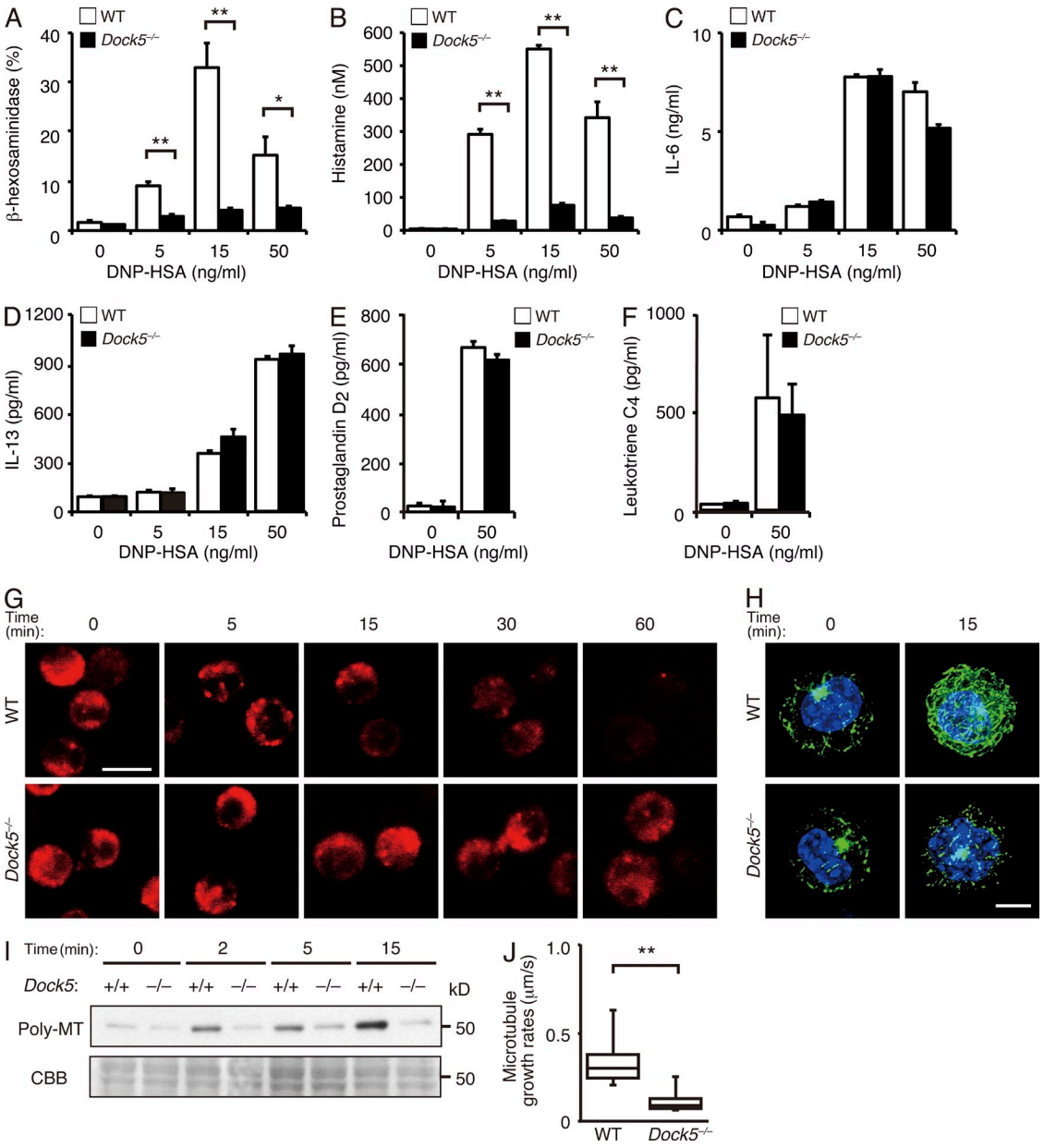

Figure 3. DOCK5 regulates mast cell degranulation by controlling microtubule dynamics. (A) Release of β-hexosaminidase from IgE-sensitized WT and *Dock5*$^{-/-}$ BMMCs was measured with *p*-nitrophenyl-*N*-acetyl-β-D-glucosaminide 1 h after stimulation with the indicated concentration of DNP-HSA. (B) Release of histamine from IgE-sensitized WT and *Dock5*$^{-/-}$ BMMCs was measured by ELISA 1 h after stimulation with the indicated concentration of DNP-HSA. (A and B) Data (mean ± SD of triplicate samples) are representative of four independent experiments; *, $P < 0.05$; **, $P < 0.01$. (C and D) Production of IL-6 (C) or IL-13 (D) by IgE-sensitized WT and *Dock5*$^{-/-}$ BMMCs was measured by ELISA 3 h after stimulation with the indicated concentration of DNP-HSA. Data (mean ± SD of triplicate samples) are representative of three (C) or four (D) independent experiments. (E and F) Production of prostaglandin D_2 (E) or leukotriene C_4 (F) by IgE-sensitized WT and *Dock5*$^{-/-}$ BMMCs was measured by ELISA 1 h (E) or 15 min (F) after stimulation with DNP-HSA. Data (mean ± SD of triplicate samples) are representative of two (E) or three (F) independent experiments. (G) Secretory granules in WT and *Dock5*$^{-/-}$ BMMCs were visualized with LysoTracker at the indicated time points after stimulation with anti-DNP IgE plus DNP-HSA. (H) Organization of microtubules in WT and *Dock5*$^{-/-}$ BMMCs was visualized by microscopy at the indicated time points after stimulation with anti-DNP IgE plus DNP-HSA. Cells were stained for tubulin (green) and nuclei (blue). (G and H) Data are representative of five (G) or four (H) independent experiments. Bars: (G) 10 µm; (H) 5 µm. (I) IgE-sensitized WT and *Dock5*$^{-/-}$ BMMCs were stimulated with DNP-HSA for the indicated times and then lysed. Polymeric tubulin in the Triton-insoluble fraction was detected with anti–α-tubulin antibody (top), and an SDS-PAGE containing Triton-soluble proteins was stained with CBB (bottom). Data are representative of two independent experiments. (J) Box plot depicts microtubule growth rates in the cell periphery in WT ($n = 10$) and *Dock5*$^{-/-}$ ($n = 12$) BMMCs stimulated with anti-DNP IgE plus DNP-HSA. Growing ends of microtubules were visualized with GFP-tagged c-APC. Data were collected from four separate experiments, and microtubule growth rates were measured in each cell at three to four different points. Each box plot exhibits the median (central line within each box), the 25th and 75th percentile values (box ends), and the 10th and 90th percentile values (error bars). Data are representative of two sets of independent analyses; **, $P < 0.01$.

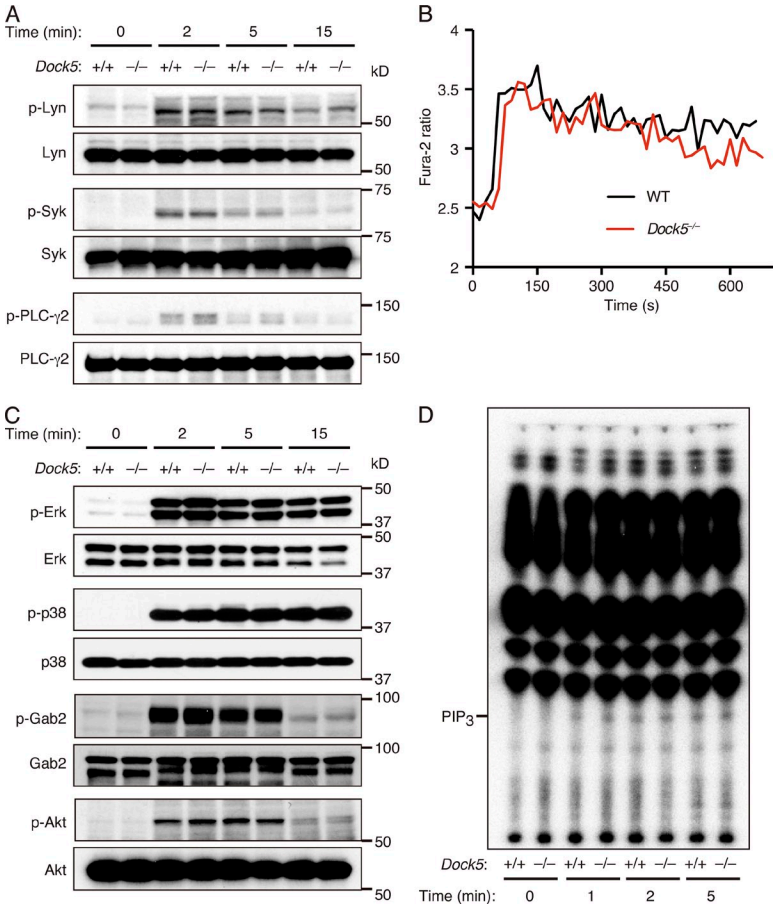

Figure 4. Effect of DOCK5 deficiency on FcεRI-mediated proximal signaling. (A) IgE-sensitized WT and *Dock5*$^{-/-}$ BMMCs were stimulated with DNP-HSA for the indicated times, lysed, and analyzed by immunoblot for phosphorylated and total Lyn, Syk, and PLC-γ2. Data are representative of two (for Lyn and PLC-γ2) or three (for Syk) independent experiments. (B) IgE-sensitized WT and *Dock5*$^{-/-}$ BMMCs were loaded with Fura2-AM, suspended with Tyrode's buffer, and stimulated with DNP-HSA. Data are indicated as the Fura-2 ratio at 340:380 nm and are representative of five independent experiments. (C) IgE-sensitized WT and *Dock5*$^{-/-}$ BMMCs were stimulated with DNP-HSA for the indicated times, lysed, and analyzed by immunoblot for phosphorylated and total Erk, p38, Gab2, and Akt. Data are representative of two (for Erk, p38, and Akt) or three (for Gab2) independent experiments. (D) IgE-sensitized WT and *Dock5*$^{-/-}$ BMMCs were labeled with $^{32}P_i$ and stimulated with DNP-HSA. Phospholipids were extracted at the indicated times and separated on a thin-layer chromatography plate for PIP_3 measurement. Data are representative of two independent experiments.

(Fig. 3 G). However, although the LysoTracker dye rapidly disappeared in WT BMMCs upon stimulation with DNP-HSA, secretory granules were retained in cytoplasm for longer times in the case of *Dock5*$^{-/-}$ BMMCs (Fig. 3 G), suggesting that DOCK5 regulates movement of secretory granules. Intracellular trafficking of secretory granules depends on microtubule dynamics (Martin-Verdeaux et al., 2003; Smith et al., 2003; Nishida et al., 2005; Dráber et al., 2012). When IgE-sensitized WT BMMCs were stimulated with DNP-HSA, the intensity of tubulin staining was enhanced and network formation was detected (Fig. 3 H). However, such microtubule formation was severely impaired in *Dock5*$^{-/-}$ BMMCs (Fig. 3 H). Consistent with this finding, the amount of polymeric tubulin was markedly reduced in *Dock5*$^{-/-}$ BMMCs, as compared with that in WT BMMCs (Fig. 3 I).

To examine to what extent DOCK5 deficiency affects microtubule dynamics, we expressed GFP-tagged C-terminal fragment of adenomatous polyposis coli (c-APC), a molecular probe to detect the growing ends of microtubules (Mimori-Kiyosue et al., 2000), in WT and *Dock5*$^{-/-}$ BMMCs and measured microtubule growth rates (Video 1). We found that DOCK5 deficiency reduces the growth speed of microtubules to 32% of the WT level (0.357 vs. 0.116 µm/s; Fig. 3 J). These results indicate that DOCK5 controls mast cell degranulation by regulating microtubule dynamics.

DOCK5 regulates mast cell degranulation through association with Nck2

To explore the mechanism by which DOCK5 regulates microtubule dynamics and degranulation in mast cells, we first analyzed phosphorylation and activation of signaling molecules downstream of FcεRI. Upon cross-linking of FcεRI, Lyn, Syk, and PLC-γ2 were comparably phosphorylated between WT and *Dock5*$^{-/-}$ BMMCs (Fig. 4 A). Consistent with this finding, FcεRI-mediated calcium influx was intact in *Dock5*$^{-/-}$ BMMCs (Fig. 4 B). Similarly, phosphorylations of Erk, p38, Gab2, and Akt as well as production of phosphatidylinositol 3,4,5-triphosphate (PIP_3) were unchanged between WT and *Dock5*$^{-/-}$ BMMCs (Fig. 4, C and D). These results indicate that canonical signaling cascades important for mast cell functions operate normally even in the absence of DOCK5.

Several lines of evidence indicate that microtubule dynamics are regulated directly or indirectly by small GTPases (Etienne-Manneville and Hall, 2002). Although DOCK5 acts as a Rac GEF (Côté and Vuori, 2006; Sanematsu et al., 2013), FcεRI-mediated Rac activation was unchanged between WT and *Dock5*$^{-/-}$ BMMCs (Fig. 5 A). To determine the functional domain of DOCK5 critical for mast cell degranulation, we expressed several mutants of GFP-fusion DOCK5 (GFP-DOCK5) in *Dock5*$^{-/-}$ BMMCs by adenoviral transfer (Fig. 5 B). By analogy to the DOCK2 DHR-2 domain

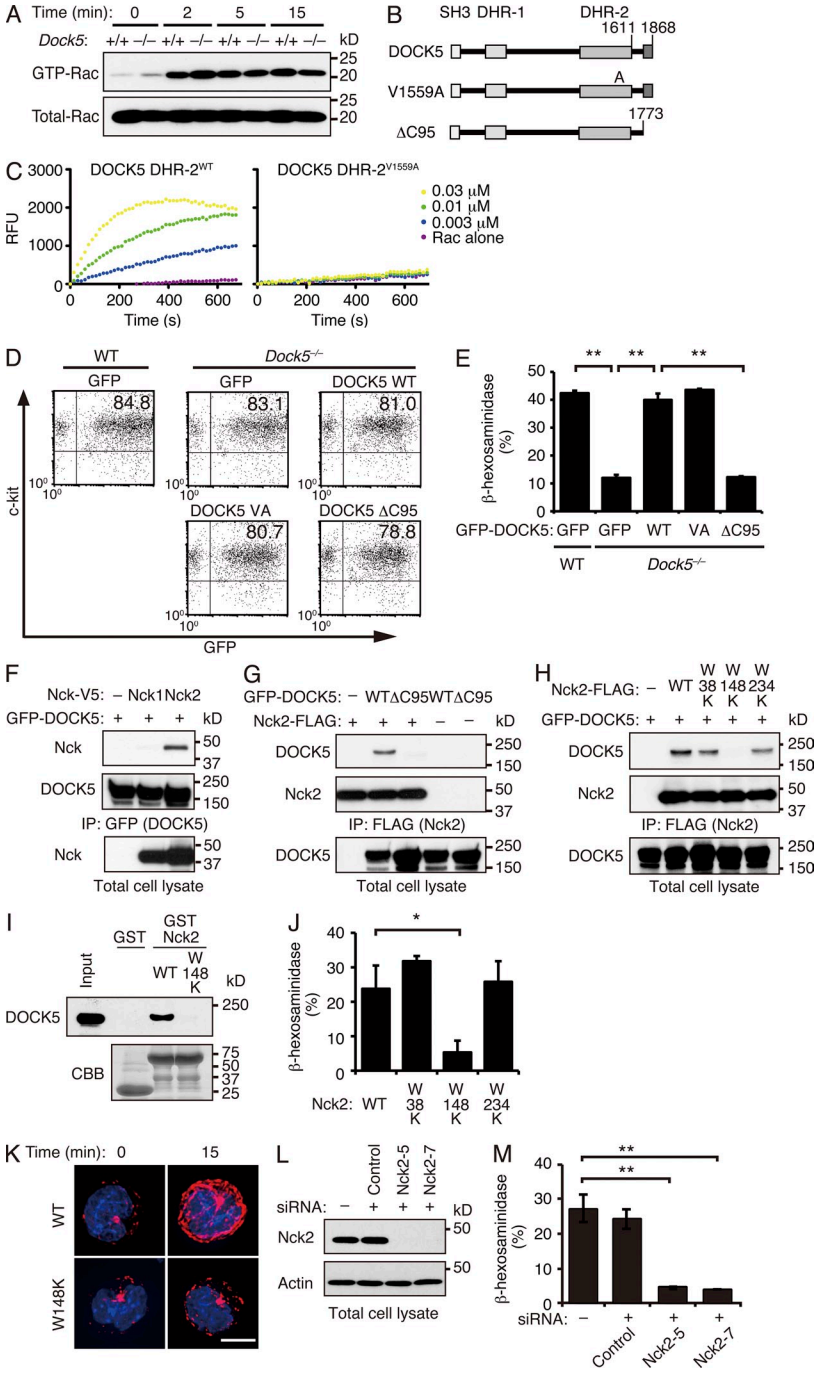

Figure 5. DOCK5 regulates mast cell degranulation through association with Nck2.
(A) IgE-sensitized WT and *Dock5*$^{-/-}$ BMMCs were stimulated with DNP-HSA for the indicated times and lysed. Aliquots of the cell extracts were kept for total lysate control, and the remaining extracts were incubated with GST-fusion Rac-binding domain of PAK1. The bound proteins and the total lysate control were probed by immunoblot with anti-Rac1 antibody. Data are representative of five independent experiments. (B) Schematic representation of DOCK5 mutants used in this experiment. (C) Recombinant WT (DHR-2^{WT}) and mutant (DHR-2^{V1559A}) DOCK5 DHR-2 proteins were incubated with GDP-loaded GST-fusion Rac1 in the presence of BODIPY-FL-GTP. The change of BODIPY-FL fluorescence was monitored to measure the level of GTP–GDP exchange reaction. Data are representative of two independent experiments. RFU, relative fluorescence unit. (D) The expression of GFP-tagged WT and mutant DOCK5 in *Dock5*$^{-/-}$ BMMCs was measured by flow cytometry after adenoviral transfer. As a control, WT BMMCs expressing GFP alone were also analyzed. Data are representative of six independent experiments. VA, V1559A mutant. (E) Release of β-hexosaminidase from *Dock5*$^{-/-}$ BMMCs expressing WT or mutant DOCK5 was measured with *p*-nitrophenyl-*N*-acetyl-β-D-glucosaminide 1 h after stimulation with anti-DNP IgE plus DNP-HSA. As a control, WT BMMCs expressing GFP alone were also analyzed. Data (mean ± SD of triplicate samples) are representative of six independent experiments; **, $P < 0.01$. (F) After expression of GFP-tagged DOCK5 in HEK-293T cells with V5-tagged Nck1 or Nck2, cell extracts were immunoprecipitated with anti-GFP antibody. The precipitated proteins (top and middle) and total lysate control (bottom) were analyzed by immunoblot for Nck1, Nck2, or DOCK5. (G) After expression of FLAG-tagged Nck2 in HEK-293T cells with GFP-tagged WT or mutant DOCK5, cell extracts were immunoprecipitated with anti-FLAG antibody. The precipitated proteins (top and middle) and total lysate control (bottom) were analyzed by immunoblot for DOCK5 or Nck2. (H) After expression of GFP-tagged DOCK5 in HEK-293T cells with FLAG-tagged WT or mutant Nck2, cell extracts were immunoprecipitated with anti-FLAG antibody. The precipitated proteins (top and middle) and total lysate control (bottom) were analyzed by immunoblot for DOCK5 or Nck2. (F–H) Data are representative of three (F and H) or eight (G) independent experiments. (I) The MC/9 cell lysates were pulled down with GST alone or GST-fusion Nck2 (WT and W148K mutant), and the bound proteins and total lysate control (input) were probed by immunoblot with anti-DOCK5 antibody (top). The recombinant proteins used in this assay were detected with CBB staining (bottom). Data are representative of two independent experiments. (J) Release of β-hexosaminidase from MC/9 cells stably expressing WT or mutant Nck2 was measured with *p*-nitrophenyl-*N*-acetyl-β-D-glucosaminide 1 h after stimulation with anti-DNP IgE plus DNP-HSA. Data (mean ± SD of triplicate samples) are representative of two independent experiments; *, $P < 0.05$. (K) Organization of microtubules in MC/9 cells stably expressing WT or mutant Nck2 was visualized by microscopy at the indicated time points after stimulation with anti-DNP IgE plus DNP-HSA. Cells were stained for tubulin (red) and nuclei (blue). Data are representative of two independent experiments. Bar, 5 μm. (L) MC/9 cells were treated with siRNAs (Nck2-5 and Nck2-7) or control oligonucleotide, lysed, and analyzed by immunoblot for Nck2 or actin as a control. Data are representative of three independent experiments. (M) Release of β-hexosaminidase from Nck2-knocked down MC/9 cells was measured with *p*-nitrophenyl-*N*-acetyl-β-D-glucosaminide 1 h after stimulation with anti-DNP IgE plus DNP-HSA. Data (mean ± SD of triplicate samples) are representative of two independent experiments; **, $P < 0.01$.

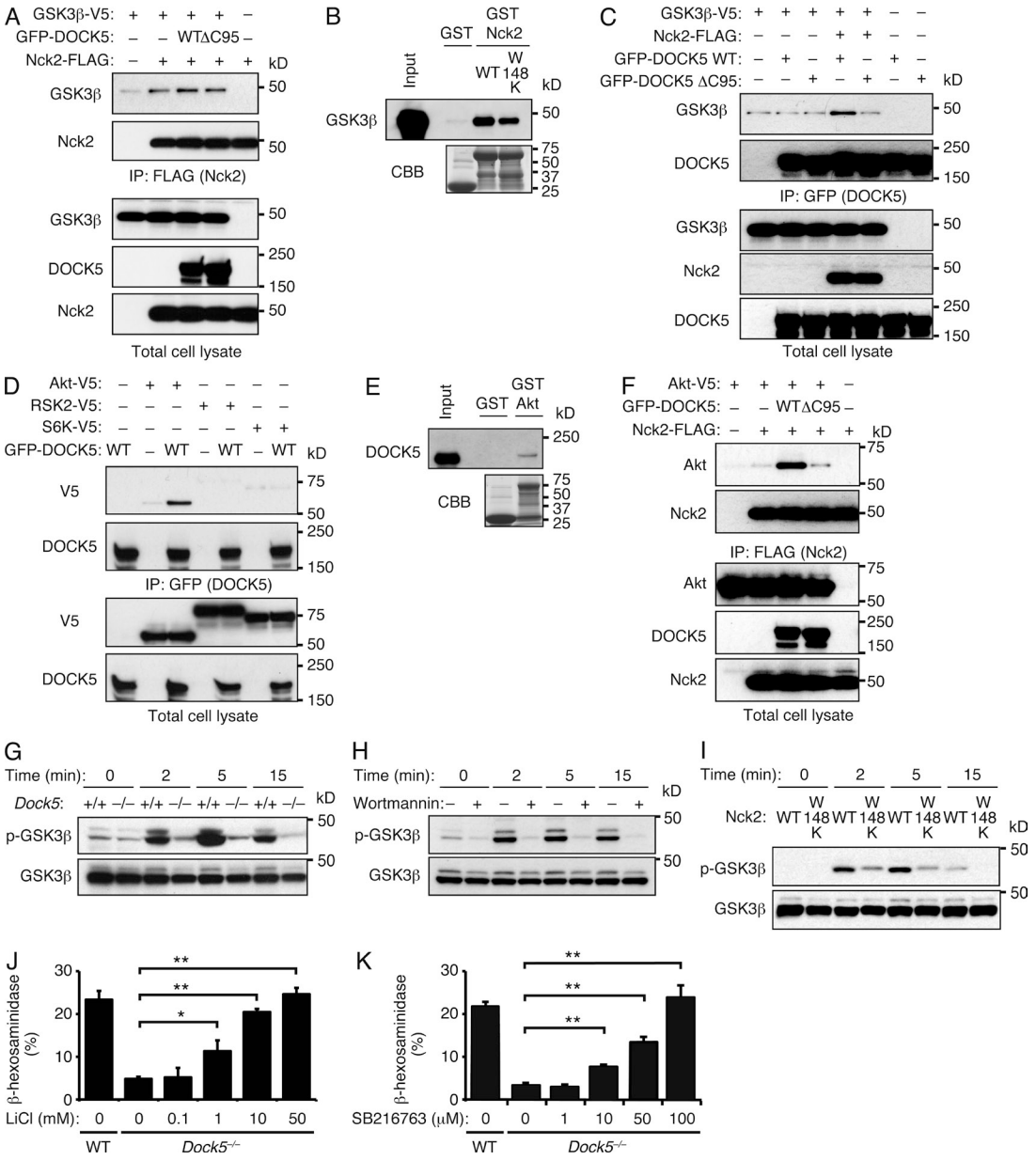

Figure 6. DOCK5 acts as an adaptor to mediate phosphorylation and inactivation of GSK3β. (A) After expression of FLAG-tagged Nck2 and/or V5-tagged GSK3β in HEK-293T cells with GFP-tagged WT or mutant DOCK5, cell extracts were immunoprecipitated with anti-FLAG antibody. The precipitated proteins (top two panels) and total lysate control (bottom three panels) were analyzed by immunoblot for GSK3β, Nck2, or DOCK5. (B) The MC/9 cell lysates were pulled down with GST alone or GST-fusion Nck2 (WT and W148K mutant), and the bound proteins and total lysate control (input) were probed by immunoblot with anti-GSK3β antibody (top). The recombinant proteins used in this assay were detected with CBB staining (bottom). (C) After expression of GFP-tagged WT or mutant DOCK5 in HEK-293T cells with FLAG-tagged Nck2 and/or V5-tagged GSK3β, cell extracts were immunoprecipitated with anti-GFP antibody. The precipitated proteins (top two panels) and total lysate control (bottom three panels) were analyzed by immunoblot for GSK3β, DOCK5, and Nck2. (A–C) Data are representative of six (A), two (B), or four (C) independent experiments. (D) After expression of GFP-tagged WT DOCK5 in HEK-293T cells with V5-tagged Akt, RSK2, or S6K, cell extracts were immunoprecipitated with anti-GFP antibody. The precipitated proteins (top two panels) and total lysate control (bottom two panels) were analyzed by immunoblot for DOCK5 or V5-tagged proteins. (E) The MC/9 cell lysates were pulled down with GST alone or GST-fusion Akt, and the bound proteins and total lysate control (input) were probed by immunoblot with anti-DOCK5 antibody (top). The recombinant proteins used in this assay were detected with CBB staining (bottom). (F) After expression of FLAG-tagged Nck2 and/or V5-tagged Akt in HEK-293T cells with GFP-tagged WT or mutant DOCK5, cell extracts were immunoprecipitated with anti-FLAG antibody. The precipitated proteins (top two panels) and total lysate control (bottom three panels) were analyzed by immunoblot for Akt, Nck2, or DOCK5. (D–F) Data are representative of three (D), two (E), or five (F) independent experiments. (G) IgE-sensitized WT and *Dock5*$^{-/-}$ BMMCs were stimulated with DNP-HSA for the indicated times, lysed, and analyzed by immunoblot for phosphorylated and total GSK3β. (H) GSK3β phosphorylation in WT BMMCs treated with 100 nM wortmannin was assayed by immunoblot. Total GSK3β is show as a control. (I) IgE-sensitized

(Kulkarni et al., 2011), the valine residue at position 1559 of DOCK5 was expected to function as a nucleotide sensor. Indeed, when this valine was mutated to alanine, the Rac GEF activity of DOCK5 DHR-2 was completely lost (Fig. 5 C). However, the expression of this GEF-dead DOCK5 mutant (V1559A) completely restored degranulation response of *Dock5*$^{-/-}$ BMMCs (Fig. 5, D and E), indicating that DOCK5 regulates mast cell degranulation independently of its Rac GEF activity. Unlike DOCK2, DOCK5 encodes canonical proline-rich sequences at its C terminus that are likely to bind to the Src homology 3 (SH3) domains. When the C-terminal 95 amino acid residues (1774 to 1868) containing the proline-rich sequences were deleted from DOCK5 (Fig. 5 B), this ΔC95 mutant failed to rescue the degranulation defect in *Dock5*$^{-/-}$ BMMCs (Fig. 5, D and E).

We next searched for the binding partner of the C-terminal region of DOCK5 necessary to transmit the signal for mast cell degranulation. Nck1 and Nck2 form a family of ubiquitously expressed adaptor proteins comprising primarily three N-terminal SH3 domains and one C-terminal SH2 domain (Li et al., 2001). We found that DOCK5 binds to Nck2, but not Nck1, by expressing these constructs in human embryonic kidney 293T (HEK-293T) cells (Fig. 5 F). As this binding was completely abolished by deleting the C-terminal 95 amino acid residues of DOCK5 (ΔC95; Fig. 5 G), it seemed likely that Nck2 associates with DOCK5 through the SH3 domain. Indeed, the association between DOCK5 and Nck2 was abolished by mutating the tryptophan residue located in the center of the second SH3 domain of Nck2 to lysine (designated W148K; Fig. 5 H). Similar results were obtained when cell lysates of the mast cell line MC/9 were subjected to pull-down assays with glutathione *S*-transferase (GST)–fusion recombinant protein encoding WT Nck2 or W148K mutant (Fig. 5 I). In contrast, inactivation of the first or third SH3 domain of Nck2 (W38K or W234K) did not affect DOCK5 binding (Fig. 5 H). These results indicate that Nck2 associates with DOCK5 through the second SH3 domain.

To reveal the functional significance of this interaction, we first expressed WT or mutant Nck2 in the mast cell line MC/9. When MC/9 cells stably expressing WT Nck2 were sensitized with anti-DNP IgE antibody and stimulated with DNP-HSA, 20–30% of the total amount of β-hexosaminidase was released (Fig. 5 J). However, the expression of W148K, but not W38K and W234K, in MC/9 cells markedly suppressed FcεRI-mediated β-hexosaminidase release (Fig. 5 J), suggesting that the W148K mutant acts in a dominant-negative manner. Consistent with this, microtubule formation after FcεRI cross-linking was hardly detected in MC/9 cells expressing W148K mutant (Fig. 5 K). In addition, we found that FcεRI-mediated degranulation was severely impaired in MC/9 cells by knocking down Nck2 expression using siRNA (Fig. 5, L and M). Collectively, these results indicate that the association between DOCK5 and Nck2 is essential for mast cell degranulation.

DOCK5 forms a novel multimolecular complex to phosphorylate and inactivate GSK3β

During the course of screening for Nck2-binding proteins, we found that Nck2 and GSK3β were coimmunoprecipitated when expressed in HEK-293T cells (Fig. 6 A). As this association was detected irrespective of the presence of DOCK5 (Fig. 6 A), it was suggested that Nck2 itself associates with GSK3β. Indeed, GSK3β was pulled down from MC/9 cell lysates with GST-fusion WT Nck2 and its mutant W148K (Fig. 6 B). In line with this finding, GSK3β was immunoprecipitated with WT DOCK5, but not with ΔC95 mutant, only when Nck2 was also coexpressed (Fig. 6 C). Although GSK3β is phosphorylated at Ser9 by serine/threonine kinases such as Akt, p90 ribosomal S6 kinase (RSK), and p70 S6 kinase (S6K; Cohen and Frame, 2001), DOCK5 was immunoprecipitated with Akt, but not with RSK and S6K (Fig. 6 D). The significant, albeit weak, binding between DOCK5 and Akt was also observed in a pull-down assay using MC/9 cell lysates (Fig. 6 E). When Akt and Nck2 were expressed with WT DOCK5 or ΔC95 mutant, Akt and Nck2 were coimmunoprecipitated only in the presence of WT DOCK5 (Fig. 6 F). Thus, DOCK5 forms a complex with Akt, Nck2, and GSK3β.

To examine the physiological function of this multimolecular complex, we compared FcεRI-mediated GSK3β phosphorylation between WT and *Dock5*$^{-/-}$ BMMCs. After cross-linking of FcεRI, GSK3β was phosphorylated at Ser9 in WT BMMCs (Fig. 6 G). However, GSK3β phosphorylation was severely impaired in *Dock5*$^{-/-}$ BMMCs as well as WT BMMCs treated with the PI3K inhibitor wortmannin (Fig. 6, G and H). A similar defect was observed when MC/9 cells stably expressing the Nck2 mutant W148K were analyzed (Fig. 6 I). In addition, we found that degranulation defect of *Dock5*$^{-/-}$ BMMCs was rescued by treating them with the GSK3β inhibitor lithium chloride (LiCl; Klein and Melton, 1996) and SB216763 (Coghlan et al., 2000; Fig. 6, J and K). Collectively, these results indicate that DOCK5 associates with Nck2 and Akt and regulates mast cell degranulation through phosphorylation and inactivation of GSK3β.

DISCUSSION

Cross-linking of FcεRI on mast cells with IgE and antigens initiates signals leading to the release of chemical mediators that induce anaphylactic responses. Although much is known

MC/9 cells stably expressing WT or mutant Nck2 were stimulated with DNP-HSA for the indicated times, lysed, and analyzed by immunoblot for phosphorylated and total GSK3β. (G–I) Data are representative of four (G), three (H), or five (I) independent experiments. (J and K) IgE-sensitized *Dock5*$^{-/-}$ BMMCs were treated with various concentrations of LiCl (J) or SB216763 (K) and were then stimulated with DNP-HSA for 1 h before β-hexosaminidase release assays. As a control, WT BMMCs treated with vehicle alone (H_2O for LiCl and DMSO for SB216763) were similarly analyzed. Data (mean ± SD of triplicate samples) are representative of five independent experiments; *, $P < 0.05$; **, $P < 0.01$.

about proximal signals downstream of FcεRI (Alvarez-Errico et al., 2009; Gilfillan and Rivera, 2009; Kambayashi et al., 2009), the distal mechanism controlling mast cell degranulation is poorly understood. Here we provide evidence that DOCK5 regulates FcεRI-mediated mast cell degranulation in vitro and anaphylactic responses in vivo. Although FcεRI-mediated proximal signaling events, including activation of tyrosine kinases and induction of calcium influx, occurred normally even in the absence of DOCK5, microtubule rearrangement and movement of secretory granules were defective in *Dock5*$^{-/-}$ BMMCs. Our results thus identify DOCK5 as a critical regulator of microtubule dynamics during mast cell degranulation.

Although DOCK5 acts as a Rac GEF (Côté and Vuori, 2006; Sanematsu et al., 2013), rescue experiments in DOCK5-null mast cells revealed that the Rac GEF activity of DOCK5 is not required for mast cell degranulation. Instead, we found that DOCK5 regulates mast cell degranulation through the association with Nck2. So far, many proteins that directly influence the actin polymerization machinery, such as Wiskott-Aldrich syndrome protein (WASP), p21-activated kinase 1 (PAK1), and WASP-interacting protein (WIP), have been reported to bind to Nck (Li et al., 2001). However, although calcium mobilization, cytokine production, and/or PLC-γ phosphorylation was impaired in WASP-, PAK1-, or WIP-deficient BMMCs (Pivniouk et al., 2003; Kettner et al., 2004; Allen et al., 2009), these signaling events were intact in *Dock5*$^{-/-}$ BMMCs. Therefore, it is suggested that DOCK5 regulates mast cell degranulation independently of a WASP-, PAK1-, or WIP-mediated pathway.

GSK3β is a serine/threonine kinase that negatively regulates microtubule dynamics (Cohen and Frame, 2001; Zhou and Snider, 2005). In resting cells, GSK3β phosphorylates microtubule-binding proteins and inhibits their ability to promote microtubule assembly (Zhou et al., 2004; Yoshimura et al., 2005; Kim et al., 2011). However, this inhibitory effect is relieved when GSK3β is phosphorylated at Ser9 (Cohen and Frame, 2001). In this study, we have shown that DOCK5 forms a complex with GSK3β through the interaction with Nck2. When this complex formation was blocked, FcεRI-mediated GSK3β phosphorylation at Ser9 was impaired, resulting in a marked reduction in microtubule dynamics and a severe defect in degranulation. Conversely, the defect in degranulation of *Dock5*$^{-/-}$ BMMCs was rescued by treating them with the GSK3β inhibitors. These results indicate that the DOCK5–Nck2 axis regulates mast cell degranulation through phosphorylation and inactivation of GSK3β.

Previous studies have indicated that the Fyn–Gab2–PI3K pathway plays a key role in translocation of secretory granules (Parravicini et al., 2002; Nishida et al., 2005, 2011). However, downstream targets of PI3K activation remain to be determined. One such target may be GSK3β because treatment of WT BMMCs with the PI3K inhibitor suppressed FcεRI-mediated GSK3β phosphorylation at Ser9. As FcεRI-mediated Gab2 phosphorylation and PIP_3 production were unchanged between WT and *Dock5*$^{-/-}$ BMMCs, it is clear that the Fyn–Gab2–PI3K pathway normally operates even in the absence of DOCK5. Nonetheless, FcεRI-mediated GSK3β phosphorylation was severely impaired in *Dock5*$^{-/-}$ BMMCs. We found that DOCK5 also interacts with Akt, a serine/threonine kinase which phosphorylates GSK3β in a manner dependent on PI3K activation (Cohen and Frame, 2001). Therefore, it is likely that DOCK5 acts as a signaling hub to facilitate GSK3β phosphorylation by Akt and to promote microtubule assembly during mast cell degranulation.

In conclusion, we have demonstrated that DOCK5 associates with Nck2 and Akt and regulates microtubule dynamics and mast cell degranulation through phosphorylation and inactivation of GSK3β. As *Dock5*$^{-/-}$ mice exhibit resistance to systemic and cutaneous anaphylaxis without showing any fetal defects, DOCK5 may be a novel therapeutic target for controlling type I allergic responses.

MATERIALS AND METHODS

Mice. *Dock2*$^{-/-}$, *Dock5*$^{-/-}$, and *Kit*$^{W\text{-}sh/W\text{-}sh}$ C57BL/6 (provided by S. Koyasu, RIKEN Center for Integrative Medical Sciences, Yokohama, Japan) mice have been described previously (Lyon and Glenister, 1982; Duttlinger et al., 1993; Fukui et al., 2001; Laurin et al., 2008). *Dock2*$^{-/-}$ and *Dock5*$^{-/-}$ mice were backcrossed onto a C57BL/6 background for more than eight generations before use, and age- and sex-matched C57BL/6 mice were used as WT controls. Mice were kept under specific pathogen–free conditions in the animal facility of Kyushu University. The committee of Ethics of Animal Experiments at Kyushu University approved all animal experiments performed in this study.

Cell culture. For preparation of BMMCs, 6–8-wk-old mice were sacrificed and their BM cells were cultured in RPMI 1640 medium supplemented with 10% heat-inactivated FCS, 100 U/ml penicillin, 0.1 mg/ml streptomycin, 50 μM 2-ME, and 5 ng/ml IL-3 (PeproTech). The medium was changed every 3–4 d during culture. After 4–5 wk of culture, cells were stained to monitor surface expression of FcεRI and c-kit before use. MC/9 cells were obtained from the ATCC and maintained in DMEM supplemented with 10% heat-inactivated FCS, 100 U/ml penicillin, 0.1 mg/ml streptomycin, 50 μM 2-ME, and 10% T-STIM with ConA (BD).

Passive systemic anaphylaxis. WT and *Dock5*$^{-/-}$ mice were sensitized by intravenously injecting 10 μg anti-DNP mouse IgE antibody (SPE-7; Sigma-Aldrich) 24 h before intravenous administration of 100 μg DNP-HSA (Sigma-Aldrich). After antigen challenge, rectal temperatures were measured every 5 min for 30 min with a digital thermometer (Physitemp Instruments). Mice were then sacrificed and peripheral blood was taken by cardiac puncture to measure serum concentration of histamine with an ELISA kit (SPI-BIO).

Passive cutaneous anaphylaxis. WT and *Dock5*$^{-/-}$ mice were passively sensitized by intravenously injecting 2 μg anti-DNP mouse IgE antibody. Then, 24 h later, mice were challenged by epicutaneous application of acetone/olive oil (4:1) alone to the right ear and 20 μl DNFB (0.6% wt/vol) in acetone and olive oil to the left ear. Ear-swelling responses were assessed by measurement of ear thickness with a digital thickness gauge (model 293-230; Mitutoyo). Net ear swelling was calculated as the difference in the thickness of the right and left ear.

Mast cell reconstitution. Mast cell reconstitution of *Kit*$^{W\text{-}sh/W\text{-}sh}$ mice was performed as described previously (Grimbaldeston et al., 2005; Wolters et al., 2005). In brief, 10^7 WT or *Dock5*$^{-/-}$ BMMCs were injected into the tail vein of 6–7-wk-old *Kit*$^{W\text{-}sh/W\text{-}sh}$ mice. 11 wk after injection, mice were sacrificed and tissues were stained with toluidine blue to assess reconstitution

efficiencies. In separate experiments, reconstituted *Kit*$^{W\text{-}sh/W\text{-}sh}$ mice were sensitized with anti-DNP mouse IgE antibody and challenged with DNP-HSA for induction of passive systemic anaphylaxis.

RT-PCR. RNA samples were treated with RNase-free DNase I (Invitrogen), were reverse-transcribed with oligo(dT) and SuperScript III reverse transcriptase (Invitrogen), and were amplified by PCR with specific primers described previously (Morii et al., 1997).

Degranulation assay. 10^5 BMMCs and 10^5 MC/9 transfectants were sensitized for 3 h at 37°C with 1 μg/ml anti-DNP IgE antibody and were stimulated for 1 h with various concentrations of DNP-HSA in Tyrode's buffer (130 mM NaCl, 5 mM KCl, 1.4 mM $CaCl_2$, 1 mM $MgCl_2$, 5.6 mM glucose, 0.1% BSA, and 10 mM Hepes, pH 7.4). Where indicated, cells were treated with LiCl (Wako Chemicals), SB216763 (Sigma-Aldrich), or vehicle (H_2O or DMSO) for 30 min before stimulation with DNP-HSA. Samples were centrifuged, and supernatant was collected to measure the released β-hexosaminidase and histamine. To determine the total cell content of β-hexosaminidase, cells were lysed with 0.5% (vol/vol) Triton X-100 in Tyrode's buffer. For degranulation assay, 100 μl of supernatants or cell lysates was incubated with 50 μl *p*-nitrophenyl-*N*-acetyl-β-D-glucosaminide (1.3 mg/ml in 0.1 M sodium citrate, pH 4.5; Sigma-Aldrich), and color was developed for 60 min at 37°C. The reaction was stopped by the addition of 150 μl of 0.2 M glycine-NaOH, pH 10.7, and absorbance at 405 nm was measured with a microplate reader. Total amount of β-hexosaminidase was comparable between WT and *Dock5*$^{-/-}$ BMMCs (absorbance at 405 nm: WT 1.50 ± 0.15 vs. *Dock5*$^{-/-}$ 1.56 ± 0.05; $n = 3$). Percent degranulation was calculated as follows: absorbance of culture supernatants at 405 nm × 100/absorbance of total cell lysate at 405 nm.

Measurement of cytokines and lipid mediators. BMMCs were stimulated as described above. The cell culture supernatants were harvested 3 h after stimulation, and concentrations of IL-6 and IL-13 were measured with ELISA kits (from Thermo Fisher Scientific and R&D Systems). Concentrations of prostaglandin D_2 and leukotriene C_4 in cell culture supernatants were measured at 1 h and 15 min after stimulation, respectively, using ELISA kits (both from Cayman Chemical) according to the manufacturer's instructions.

Immunofluorescence microscopy and time-lapse imaging. IgE-sensitized BMMCs were stained for 20 min at 37°C with LysoTracker red (Molecular Probes) for visualization of secretory lysosome. After stimulation with 15 ng/ml DNP-HSA, images were taken with a laser-scanning confocal microscope (LSM510 META; Carl Zeiss). For tubulin staining, BMMCs stimulated with 15 ng/ml DNP-HSA were fixed with 4% paraformaldehyde, permeabilized with 0.1% Triton X-100 in PBS, blocked with 1% BSA in PBS, and stained with anti–α-tubulin antibody (DM1A; EMD Millipore) and DAPI (Wako Chemicals). The DeltaVision Restoration Microscopy system (Applied Precision) with a 100× objective attached to a cooled charge-coupled device camera was used for microscopy. Images were acquired with the DeltaVision softWoRx Resolve 3D capture program and were collected as a stack of 0.2-μm increments in the z axis. To quantitatively analyze microtubule dynamics, BMMCs expressing GFP-tagged c-APC were sensitized with anti-DNP IgE antibody and stimulated with 50 ng/ml DNP-HSA. Images were taken every 2 s with the DeltaVision Restoration Microscopy system, and the dynamic behavior of c-APC at the distal end of microtubule was monitored by time-lapse imaging.

Plasmids and transfection. The genes encoding Nck1, Nck2, GSK3β, and Akt with appropriate tags were amplified by PCR and subcloned into the pcDNA vector (Invitrogen). The genes encoding GFP-tagged WT DOCK5 and its mutant were subcloned into the pCI vector (Promega) or pENTR vector (Invitrogen) with human ubiquitin C (UbC) promoter. These expression vectors were transfected into HEK-293T cells with polyethylenimine. The retroviral vector pMX was used to generate the plasmid encoding WT Nck2-IRES-GFP or mutant Nck2-IRES-GFP. These plasmids were transfected into Platinum-E packaging cells (provided by T. Kitamura, The University of Tokyo, Tokyo, Japan) using FuGENE 6 transfection reagent (Roche). The cell culture supernatants were harvested 48 h after transfection, supplemented with 5 μg/ml polybrene and 5 ng/ml IL-3, and used to infect MC/9 cells. After centrifugation at 2,000 rpm for 1 h, plates were incubated for 8 h at 32°C and for 16 h at 37°C. The adenoviral vector pAd-UbC-GFP-DOCK5 encoding GFP-fusion DOCK5 was generated by specific recombination of pENTR-UbC-GFP-DOCK5 with pAd/PL-DEST (Invitrogen). The pAd-UbC-GFP-DOCK5 with or without mutations was transfected into HEK-293A cells (Invitrogen) to amplify the recombinant adenovirus. The resultant virus was purified with cesium chloride centrifugation and was used to infect *Dock5*$^{-/-}$ BMMCs. After 48 h of incubation, viable cells were recovered using Lympholyte-M (Cedarlane Labs) for degranulation assays.

Nck2 knockdown. The siRNAs Mm_Nck2_5, SI02670787; and Mm_Nck2_7, SI02713298 were obtained from QIAGEN for knockdown of Nck2 expression, and the irrelevant oligonucleotide SI03650318 was used as a negative control. Transfection was performed according to the manufacturer's instructions. In brief, 100 μl of the 200-nM siRNA solution in serum-free DMEM was mixed with 6 μl HiPerFect transfection reagent for 10 min at room temperature. This 100-μl mixture was added drop-wise to 2×10^5 MC/9 cells suspended in 100 μl DMEM containing T-STIM. The cells were incubated for 6 h at 37°C, and DMEM containing 400 μl T-STIM was added to the culture. After 48 h of incubation, cells were harvested for degranulation assay. Knockdown efficiency was checked by immunoblotting using anti-Nck2 antibody (EMD Millipore).

Pull-down assay, immunoprecipitation, and immunoblotting. IgE-sensitized BMMCs were stimulated with 50 ng/ml DNP-HSA for specified times. To assess Rac activation, cell extracts were incubated with GST-fusion Rac-binding domain of PAK1 at 4°C for 1 h. The bound proteins were analyzed by SDS-PAGE, and blots were probed with anti-Rac1 antibody (23A8; EMD Millipore). To analyze tyrosine phosphorylation of PLC-γ2, cell extracts were immunoprecipitated with anti–PLC-γ2 antibody (Santa Cruz Biotechnology, Inc.), and the precipitates were analyzed with anti-phosphotyrosine antibody (pY99; Santa Cruz Biotechnology, Inc.). Activation of Lyn, Syk, Erk, p38, Gab2, Akt, and GSK3β were assessed with the phosphorylation-specific antibodies against Tyr396 of Lyn (EP503Y; Abcam), Tyr525/526 of Syk (C87C1; Cell Signaling Technology), Thr202/Tyr204 of Erk (D13.14.4E; Cell Signaling Technology), Thr180/Tyr182 of p38 (Cell Signaling Technology), Tyr452 of Gab2 (Cell Signaling Technology), Thr308 of Akt (Cell Signaling Technology), and Ser9 of GSK3β (D3A4; Cell Signaling Technology), respectively.

The following antibodies were used to evaluate DOCK5-mediated multimolecular complex formation in HEK-293T cells and MC/9 cells: anti-FLAG M2 antibody (Sigma-Aldrich), anti-GFP antibody (MBL), anti-HA antibody (Roche), anti-V5 antibody (Invitrogen), anti-Nck2 antibody, and anti-GSK3β antibody (BD). Polyclonal antibody against DOCK5 was produced by immunizing a rabbit with KLH-coupled synthetic peptide corresponding to the C-terminal sequence (PKARKSGILSSEPGSQ, residues 1853–1868) of mouse DOCK5. HEK-293T cell lysates were immunoprecipitated with the relevant antibodies for immunoblotting. To examine whether Nck2 or Akt associates with DOCK5, MC/9 cell lysates were incubated with GST-fusion Nck2 (WT and W148K mutant) or GST-fusion Akt at 4°C for 1 h. The bound proteins were analyzed by SDS-PAGE, and blots were probed with anti-DOCK5 antibody. The association of GSK3β with Nck2 was also examined by a pull-down assay using GST-fusion Nck2 (WT and W148K mutant). Bound proteins were eluted with 0.5 M NaCl and analyzed by SDS-PAGE, and blots were probed with anti-GSK3β antibody.

Polymeric tubulin assay. Polymeric tubulin assay was performed as previously described (Nishida et al., 2005). In brief, IgE-sensitized BMMCs were stimulated with 100 ng/ml DNP-HSA for the specified times and were

suspended in extraction buffer (0.1 M Pipes, pH 7.1, 1 mM $MgSO_4$, 1 mM EGTA, 2 M glycerol, 0.1% Triton X-100, 10 µg/ml leupeptin, 10 µg/ml aprotinin, and 0.5 mM PMSF). After incubation on ice for 15 min, cell lysates were centrifuged at 15,000 rpm for 15 min, and the supernatant containing 0.1% Triton-soluble tubulin was collected. The remaining pellet was suspended in lysis buffer (25 mM Tris-HCl, pH 7.4, 0.4 M NaCl, and 0.5% SDS), boiled for 10 min, and centrifuged for 15,000 rpm for 5 min. The polymeric tubulin-containing supernatant was subjected to SDS-PAGE, and polymeric tubulin was detected by immunoblotting with anti–α-tubulin antibody (B-7; Santa Cruz Biotechnology, Inc.). The 0.1% Triton–soluble proteins were subjected to SDS-PAGE, and the gels were stained with Coomassie brilliant blue (CBB).

Calcium flux assay. 5×10^4 IgE-sensitized BMMCs were loaded with 3 µM Fura2-AM (Wako Chemicals) for 30 min at 37°C. Cells were resuspended in Tyrode's buffer and were stimulated with 100 ng/ml DNP-HSA. Fluorescence intensities were monitored at an excitation wavelength of 340 or 380 nm and emission wavelength of 510 nm using an XS-N spectrofluorimeter (Molecular Devices).

Measurement of PIP_3. IgE-sensitized BMMCs were labeled with $^{32}P_i$ and were stimulated with 50 ng/ml DNP-HSA. Phospholipids were extracted at the specified times and separated on a thin-layer chromatography plate for determination of the radioactivity in the PIP_3 fraction.

In vitro GEF assays. The gene encoding the DOCK5 DHR-2 domain or its mutant was cloned into the pET-SUMO vector to express the fusion protein. Measurement of the Rac GEF activity was performed as described previously (Nishikimi et al., 2012). In brief, GDP-loaded GST-fusion Rac1 was incubated with BODIPY-FL-GTP (Invitrogen) for 5 min at 30°C. After equilibration, WT DOCK5 DHR-2 ($DHR2^{WT}$) or its mutant ($DHR\text{-}2^{V1559A}$) was added to the mixtures, and the change of BODIPY-FL fluorescence (excitation = 488 nm, emission = 514 nm) was monitored at 30°C using an XS-N spectrofluorimeter.

Statistical analysis. Statistical analysis was performed by using the two-tailed Student's *t* test.

Online supplemental material. Videos 1 relates to Fig. 3 J and shows the dynamic nature of the microtubule plus-end in WT, but not *Dock5*$^{-/-}$, BMMCs. Online supplemental material is available at http://www.jem.org/cgi/content/full/jem.20131926/DC1.

We thank Dr. T. Kitamura for Platinum-E packaging cells, Dr. S. Koyasu for *Kit*$^{W\text{-}sh/W\text{-}sh}$ C57BL/6 mice, and K. Motomura, M. Tanaka, A. Inayoshi, and A. Aosaka (Kyushu University, Fukuoka, Japan) for technical support and assistance.

This study was supported by the CREST program and the Strategic Japanese–Swiss Cooperative Program of Japan Science and Technology Agency, Grants-in-Aid for Scientific Research from the Ministry of Education, Culture, Sports, Science and Technology of Japan, Grants-in-Aid for Scientific Research from the Japan Society for the Promotion of Science, the Uehara Memorial Foundation, and the NOVARTIS Foundation (Japan) for the promotion of Science. J.-F. Côté holds a Senior Investigator salary award from Fonds de Recherche du Québec-Santé.

The authors declare no competing financial interests.

Submitted: 11 September 2013
Accepted: 2 May 2014

REFERENCES

Allen, J.D., Z.M. Jaffer, S.J. Park, S. Burgin, C. Hofmann, M.A. Sells, S. Chen, E. Derr-Yellin, E.G. Michels, A. McDaniel, et al. 2009. p21-activated kinase regulates mast cell degranulation via effects on calcium mobilization and cytoskeletal dynamics. *Blood*. 113:2695–2705. http://dx.doi.org/10.1182/blood-2008-06-160861

Alvarez-Errico, D., E. Lessmann, and J. Rivera. 2009. Adapters in the organization of mast cell signaling. *Immunol. Rev.* 232:195–217. http://dx.doi.org/10.1111/j.1600-065X.2009.00834.x

Blott, E.J., and G.M. Griffiths. 2002. Secretory lysosomes. *Nat. Rev. Mol. Cell Biol.* 3:122–131. http://dx.doi.org/10.1038/nrm732

Brugnera, E., L. Haney, C. Grimsley, M. Lu, S.F. Walk, A.C. Tosello-Trampont, I.G. Macara, H. Madhani, G.R. Fink, and K.S. Ravichandran. 2002. Unconventional Rac-GEF activity is mediated through the Dock180-ELMO complex. *Nat. Cell Biol.* 4:574–582.

Coghlan, M.P., A.A. Culbert, D.A. Cross, S.L. Corcoran, J.W. Yates, N.J. Pearce, O.L. Rausch, G.J. Murphy, P.S. Carter, L. Roxbee Cox, et al. 2000. Selective small molecule inhibitors of glycogen synthase kinase-3 modulate glycogen metabolism and gene transcription. *Chem. Biol.* 7:793–803. http://dx.doi.org/10.1016/S1074-5521(00)00025-9

Cohen, P., and S. Frame. 2001. The renaissance of GSK3. *Nat. Rev. Mol. Cell Biol.* 2:769–776. http://dx.doi.org/10.1038/35096075

Côté, J.F., and K. Vuori. 2002. Identification of an evolutionarily conserved superfamily of DOCK180-related proteins with guanine nucleotide exchange activity. *J. Cell Sci.* 115:4901–4913. http://dx.doi.org/10.1242/jcs.00219

Côté, J.F., and K. Vuori. 2006. In vitro guanine nucleotide exchange activity of DHR-2/DOCKER/CZH2 domains. *Methods Enzymol.* 406:41–57. http://dx.doi.org/10.1016/S0076-6879(06)06004-6

Dráber, P., V. Sulimenko, and E. Dráberová. 2012. Cytoskeleton in mast cell signaling. *Front. Immunol.* 3:130. http://dx.doi.org/10.3389/fimmu.2012.00130

Duttlinger, R., K. Manova, T.Y. Chu, C. Gyssler, A.D. Zelenetz, R.F. Bachvarova, and P. Besmer. 1993. W-sash affects positive and negative elements controlling c-kit expression: ectopic c-kit expression at sites of kit-ligand expression affects melanogenesis. *Development*. 118:705–717.

Etienne-Manneville, S., and A. Hall. 2002. Rho GTPases in cell biology. *Nature*. 420:629–635. http://dx.doi.org/10.1038/nature01148

Fukui, Y., O. Hashimoto, T. Sanui, T. Oono, H. Koga, M. Abe, A. Inayoshi, M. Noda, M. Oike, T. Shirai, and T. Sasazuki. 2001. Haematopoietic cell-specific CDM family protein DOCK2 is essential for lymphocyte migration. *Nature*. 412:826–831. http://dx.doi.org/10.1038/35090591

Gilfillan, A.M., and J. Rivera. 2009. The tyrosine kinase network regulating mast cell activation. *Immunol. Rev.* 228:149–169. http://dx.doi.org/10.1111/j.1600-065X.2008.00742.x

Gotoh, K., Y. Tanaka, A. Nishikimi, R. Nakamura, H. Yamada, N. Maeda, T. Ishikawa, K. Hoshino, T. Uruno, Q. Cao, et al. 2010. Selective control of type I IFN induction by the Rac activator DOCK2 during TLR-mediated plasmacytoid dendritic cell activation. *J. Exp. Med.* 207:721–730. http://dx.doi.org/10.1084/jem.20091776

Grimbaldeston, M.A., C.C. Chen, A.M. Piliponsky, M. Tsai, S.Y. Tam, and S.J. Galli. 2005. Mast cell-deficient *W-sash* c-*kit* mutant *Kit*$^{W\text{-}sh/W\text{-}sh}$ mice as a model for investigating mast cell biology in vivo. *Am. J. Pathol.* 167:835–848. http://dx.doi.org/10.1016/S0002-9440(10)62055-X

Gu, H., K. Saito, L.D. Klaman, J. Shen, T. Fleming, Y. Wang, J.C. Pratt, G. Lin, B. Lim, J.P. Kinet, and B.G. Neel. 2001. Essential role for Gab2 in the allergic response. *Nature*. 412:186–190. http://dx.doi.org/10.1038/35084076

Kambayashi, T., D.F. Larosa, M.A. Silverman, and G.A. Koretzky. 2009. Cooperation of adapter molecules in proximal signaling cascades during allergic inflammation. *Immunol. Rev.* 232:99–114. http://dx.doi.org/10.1111/j.1600-065X.2009.00825.x

Kawakami, T., and S.J. Galli. 2002. Regulation of mast-cell and basophil function and survival by IgE. *Nat. Rev. Immunol.* 2:773–786. http://dx.doi.org/10.1038/nri914

Kettner, A., L. Kumar, I.M. Antón, Y. Sasahara, M. de la Fuente, V.I. Pivniouk, H. Falet, J.H. Hartwig, and R.S. Geha. 2004. WIP regulates signaling via the high affinity receptor for immunoglobulin E in mast cells. *J. Exp. Med.* 199:357–368. http://dx.doi.org/10.1084/jem.20030652

Kim, Y.T., E.M. Hur, W.D. Snider, and F.Q. Zhou. 2011. Role of GSK3 signaling in neuronal morphogenesis. *Front. Mol. Neurosci.* 4:48. http://dx.doi.org/10.3389/fnmol.2011.00048

Kiyokawa, E., Y. Hashimoto, S. Kobayashi, H. Sugimura, T. Kurata, and M. Matsuda. 1998. Activation of Rac1 by a Crk SH3-binding protein, DOCK180. *Genes Dev.* 12:3331–3336. http://dx.doi.org/10.1101/gad.12.21.3331

Klein, P.S., and D.A. Melton. 1996. A molecular mechanism for the effect of lithium on development. *Proc. Natl. Acad. Sci. USA*. 93:8455–8459. http://dx.doi.org/10.1073/pnas.93.16.8455

Kraft, S., and J.P. Kinet. 2007. New developments in FcεRI regulation, function and inhibition. *Nat. Rev. Immunol.* 7:365–378. http://dx.doi.org/10.1038/nri2072

Kulkarni, K., J. Yang, Z. Zhang, and D. Barford. 2011. Multiple factors confer specific Cdc42 and Rac protein activation by dedicator of cytokinesis (DOCK) nucleotide exchange factors. *J. Biol. Chem.* 286:25341–25351. http://dx.doi.org/10.1074/jbc.M111.236455

Kunisaki, Y., A. Nishikimi, Y. Tanaka, R. Takii, M. Noda, A. Inayoshi, K. Watanabe, F. Sanematsu, T. Sasazuki, T. Sasaki, and Y. Fukui. 2006. DOCK2 is a Rac activator that regulates motility and polarity during neutrophil chemotaxis. *J. Cell Biol.* 174:647–652. http://dx.doi.org/10.1083/jcb.200602142

Laurin, M., N. Fradet, A. Blangy, A. Hall, K. Vuori, and J.F. Côté. 2008. The atypical Rac activator Dock180 (Dock1) regulates myoblast fusion in vivo. *Proc. Natl. Acad. Sci. USA.* 105:15446–15451. http://dx.doi.org/10.1073/pnas.0805546105

Li, W., J. Fan, and D.T. Woodley. 2001. Nck/Dock: an adapter between cell surface receptors and the actin cytoskeleton. *Oncogene.* 20:6403–6417. http://dx.doi.org/10.1038/sj.onc.1204782

Lundequist, A., and G. Pejler. 2011. Biological implications of preformed mast cell mediators. *Cell. Mol. Life Sci.* 68:965–975. http://dx.doi.org/10.1007/s00018-010-0587-0

Lyon, M.F., and P.H. Glenister. 1982. A new allele sash (W^{sh}) at the W-locus and a spontaneous recessive lethal in mice. *Genet. Res.* 39:315–322. http://dx.doi.org/10.1017/S001667230002098X

Martin-Verdeaux, S., I. Pombo, B. Iannascoli, M. Roa, N. Varin-Blank, J. Rivera, and U. Blank. 2003. Evidence of a role for Munc18-2 and microtubules in mast cell granule exocytosis. *J. Cell Sci.* 116:325–334. http://dx.doi.org/10.1242/jcs.00216

Meller, N., M. Irani-Tehrani, W.B. Kiosses, M.A. Del Pozo, and M.A. Schwartz. 2002. Zizimin1, a novel Cdc42 activator, reveals a new GEF domain for Rho proteins. *Nat. Cell Biol.* 4:639–647. http://dx.doi.org/10.1038/ncb835

Mimori-Kiyosue, Y., N. Shiina, and S. Tsukita. 2000. Adenomatous polyposis coli (APC) protein moves along microtubules and concentrates at their growing ends in epithelial cells. *J. Cell Biol.* 148:505–518. http://dx.doi.org/10.1083/jcb.148.3.505

Morii, E., T. Jippo, T. Tsujimura, K. Hashimoto, D.K. Kim, Y.M. Lee, H. Ogihara, K. Tsujino, H.M. Kim, and Y. Kitamura. 1997. Abnormal expression of mouse mast cell protease 5 gene in cultured mast cells derived from mutant mi/mi mice. *Blood.* 90:3057–3066.

Nishida, K., S. Yamasaki, Y. Ito, K. Kabu, K. Hattori, T. Tezuka, H. Nishizumi, D. Kitamura, R. Goitsuka, R.S. Geha, et al. 2005. FcεRI-mediated mast cell degranulation requires calcium-independent microtubule-dependent translocation of granules to the plasma membrane. *J. Cell Biol.* 170:115–126. http://dx.doi.org/10.1083/jcb.200501111

Nishida, K., S. Yamasaki, A. Hasegawa, A. Iwamatsu, H. Koseki, and T. Hirano. 2011. Gab2, via PI-3K, regulates ARF1 in FcεRI-mediated granule translocation and mast cell degranulation. *J. Immunol.* 187:932–941. http://dx.doi.org/10.4049/jimmunol.1100360

Nishikimi, A., T. Uruno, X. Duan, Q. Cao, Y. Okamura, T. Saitoh, N. Saito, S. Sakaoka, Y. Du, A. Suenaga, et al. 2012. Blockade of inflammatory responses by a small-molecule inhibitor of the Rac activator DOCK2. *Chem. Biol.* 19:488–497. http://dx.doi.org/10.1016/j.chembiol.2012.03.008

Parravicini, V., M. Gadina, M. Kovarova, S. Odom, C. Gonzalez-Espinosa, Y. Furumoto, S. Saitoh, L.E. Samelson, J.J. O'Shea, and J. Rivera. 2002. Fyn kinase initiates complementary signals required for IgE-dependent mast cell degranulation. *Nat. Immunol.* 3:741–748.

Pivniouk, V.I., S.B. Snapper, A. Kettner, H. Alenius, D. Laouini, H. Falet, J. Hartwig, F.W. Alt, and R.S. Geha. 2003. Impaired signaling via the high-affinity IgE receptor in Wiskott-Aldrich syndrome protein-deficient mast cells. *Int. Immunol.* 15:1431–1440. http://dx.doi.org/10.1093/intimm/dxg148

Rådinger, M., H.S. Kuehn, M.S. Kim, D.D. Metcalfe, and A.M. Gilfillan. 2010. Glycogen synthase kinase 3β activation is a prerequisite signal for cytokine production and chemotaxis in human mast cells. *J. Immunol.* 184:564–572. http://dx.doi.org/10.4049/jimmunol.0902931

Rådinger, M., D. Smrž, D.D. Metcalfe, and A.M. Gilfillan. 2011. Glycogen synthase kinase-3β is a prosurvival signal for the maintenance of human mast cell homeostasis. *J. Immunol.* 187:5587–5595. http://dx.doi.org/10.4049/jimmunol.1101257

Sampson, H.A., A. Muñoz-Furlong, S.A. Bock, C. Schmitt, R. Bass, B.A. Chowdhury, W.W. Decker, T.J. Furlong, S.J. Galli, D.B. Golden, et al. 2005. Symposium on the definition and management of anaphylaxis: summary report. *J. Allergy Clin. Immunol.* 115:584–591. http://dx.doi.org/10.1016/j.jaci.2005.01.009

Sanematsu, F., A. Nishikimi, M. Watanabe, T. Hongu, Y. Tanaka, Y. Kanaho, J.F. Côté, and Y. Fukui. 2013. Phosphatidic acid-dependent recruitment and function of the Rac activator DOCK1 during dorsal ruffle formation. *J. Biol. Chem.* 288:8092–8100. http://dx.doi.org/10.1074/jbc.M112.410423

Sanui, T., A. Inayoshi, M. Noda, E. Iwata, M. Oike, T. Sasazuki, and Y. Fukui. 2003. DOCK2 is essential for antigen-induced translocation of TCR and lipid rafts, but not PKC-θ and LFA-1, in T cells. *Immunity.* 19:119–129. http://dx.doi.org/10.1016/S1074-7613(03)00169-9

Schmidt, A., and A. Hall. 2002. Guanine nucleotide exchange factors for Rho GTPases: turning on the switch. *Genes Dev.* 16:1587–1609. http://dx.doi.org/10.1101/gad.1003302

Smith, A.J., J.R. Pfeiffer, J. Zhang, A.M. Martinez, G.M. Griffiths, and B.S. Wilson. 2003. Microtubule-dependent transport of secretory vesicles in RBL-2H3 cells. *Traffic.* 4:302–312. http://dx.doi.org/10.1034/j.1600-0854.2003.00084.x

Vives, V., M. Laurin, G. Cres, P. Larrousse, Z. Morichaud, D. Noel, J.F. Côté, and A. Blangy. 2011. The Rac1 exchange factor Dock5 is essential for bone resorption by osteoclasts. *J. Bone Miner. Res.* 26:1099–1110. http://dx.doi.org/10.1002/jbmr.282

Wolters, P.J., J. Mallen-St Clair, C.C. Lewis, S.A. Villalta, P. Baluk, D.J. Erle, and G.H. Caughey. 2005. Tissue-selective mast cell reconstitution and differential lung gene expression in mast cell-deficient $Kit^{W\text{-}sh}/Kit^{W\text{-}sh}$ sash mice. *Clin. Exp. Allergy.* 35:82–88. http://dx.doi.org/10.1111/j.1365-2222.2005.02136.x

Yoshimura, T., Y. Kawano, N. Arimura, S. Kawabata, A. Kikuchi, and K. Kaibuchi. 2005. GSK-3β regulates phosphorylation of CRMP-2 and neuronal polarity. *Cell.* 120:137–149. http://dx.doi.org/10.1016/j.cell.2004.11.012

Zhou, F.Q., and W.D. Snider. 2005. Cell biology. GSK-3β and microtubule assembly in axons. *Science.* 308:211–214. http://dx.doi.org/10.1126/science.1110301

Zhou, F.Q., J. Zhou, S. Dedhar, Y.H. Wu, and W.D. Snider. 2004. NGF-induced axon growth is mediated by localized inactivation of GSK-3β and functions of the microtubule plus end binding protein APC. *Neuron.* 42:897–912. http://dx.doi.org/10.1016/j.neuron.2004.05.011